Pretransition phenomena at a first-order structural phase transition

B. Ya. Sukharevskiĭ, V. G. Ksenofontov, V. L. Kovarskiĭ, A. N. Ul'yanov, and I. V. Vilkova

Physicotechnical Institute of the Academy of Sciences of the Ukrainian SSR, Donetsk

(Submitted 26 February 1984)
Zh. Eksp. Teor. Fiz. **87**, 1336–1348 (October 1984)

The Mössbauer effect in ^{57}Fe impurity atoms is used to investigate the first-order structural phase transition due to the cooperative Jahn-Teller effect in $Cu_{1-x}Fe_xSiF_6{\cdot}6H_2O$ ($x < 0.05$) solid solutions. In the neighborhood $0.9T_c < T < T_c$ of the phase transition temperature T_c pretransitional changes are observed in the resonance absorption spectra. The results permit the conjecture that in this temperature region clusters form in which the copper-centered octahedra have passed into a state of dynamic disorder. Comparison of the temperature dependence of the quadrupole splitting with the x-ray diffraction data indicates that in the initial low-symmetry phase the elements of structure move toward states which are characteristic of the high-temperature phase. A microscopic model is proposed which, in the framework of molecular field theory, gives the main characteristics of the phase transition. The order parameter here is the (mean) distortion of the $[Cu(H_2O)_6]^{2+}$ octahedra. The conclusion that there are two types of sites for the cation sublattice in the low-symmetry phase, with axial and nonaxial crystalline fields, explains the presence of two quadrupole doublets in the Mössbauer spectrum, corresponding to the particular and general sites of the low-symmetry phase. The decrease in the difference of the quadrupole splitting of $^{57}Fe^{2+}$ impurity ions in these sites at low temperatures is attributed to a decrease in the frequency of dynamic Jahn-Teller distortions of the $[Cu(H_2O)_6]^{2+}$ complexes in the particular sites of the unit cell. An empirical expression is proposed for relating the quadrupole splitting at the ^{57}Fe impurity nuclei in fluosilicate matrices of space group $R\bar{3}$ to the lattice period along the trigonal axis.

1. INTRODUCTION

Structural phase transitions of second order or of first but nearly second order are usually accompanied by precursor phenomena which find a natural explanation in terms of a continuous rearrangement of the structure of the initial phase near the critical temperature T_c. Particular interest attaches to pretransition phenomena in the case of first-order phase transitions with ordinary values of the volume discontinuity (≈ 1–3%) and thermal effect ($\approx RT_c$, where R is the universal gas constant). In the traditional approach based on the work of Gibbs, a first-order transition point is determined by the accidental intersection of the thermodynamic potentials of the phases, so that pretransition phenomena should not occur. Nevertheless, such phenomena are observed for many typical first-order phase transitions. As examples we could cite the change in the Debye-Waller factor at first-order structural phase transitions iron-cobalt and iron-manganese alloys,[1] the pretransition phenomena at the order-disorder first-order phase transition in iron-cobalt and iron-manganese alloys,[1] the pretransition phenomena at the order-disorder first-order phase transition in Cu_3Au,[2] and the anomalous increase in the specific heat near the melting temperature of metals.[3] These papers did not reveal the reason for the pretransition phenomena or elucidate the relationship between these phenomena and the character and mechanism of the phase transition. Heterophase fluctuations are frequently mentioned as pretransition phenomena,[2] but although this is probably a valid example, there are insufficient experimental grounds to support it. In the majority of cases it remains unclear what the specific nature of these fluctuations is and to what degree they correspond qualitatively to the observable effects. The premelting anomalies of the specific heat in metals also cannot be explained solely in terms of thermal vacancies, since the concentration of such vacancies ($\approx 1\%$) needed to explain the observed effect[3] is almost an order of magnitude greater than the value found by other methods.

In the present paper it is shown with the aid of the Mössbauer effect for the example of the first-order structural phase transition in solid solutions based on $CuSiF_6{\cdot}6H_2O$ that the aforementioned pretransition phenomena (the anomalous change in the lattice parameters and volume[4,5] and also in the specific heat[6] in the pretransition region) are due to the cooperative motion of the elements of structure in preparation for the phase transition.

2. STRUCTURE OF SOLID SOLUTIONS BASED ON $CuSiF_6{\cdot}6H_2O$

The crystal structures of the low-temperature[7] (PII) and high-temperature[5] (PI) phases correspond to a distorted CsCl lattice and have symmetry $R\bar{3}$. The volume discontinuity ($\approx 2\%$), the thermal effect (≈ 3 kJ/mole), and the presence of hysteresis (≈ 10 K)[4] indicate that this is a first-order transition. A symmetry analysis of the PII and PI phases has revealed the presence of a third-order invariant,[5] a circumstance which also points to a first-order character for the phase transition PI $\leftrightarrow$ PII. The structural fragments of copper fluosilicate are $[Cu(H_2O)_6]^{2+}$ and $[SiF_6]^{2-}$ octahedra arranged in columns parallel to the trigonal axis of the crystal. The cation sublattice of PII is formed by two types of copper octahedra (Fig. 1). In the unit cell of the PII phase the general sites occupied by the distorted $[Cu(H_2O)_6]^{2+}$ octahedra

0038-5646/84/100767-07$04.00

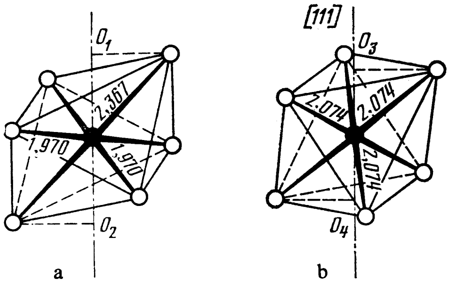

FIG. 1. The octahedral complex $[Cu(H_2O)_6]^{2+}$ in the general (a) and particular (b) sites of the unit cell of the PII phase of $CuSiF_6 \cdot 6H_2O$. The projections onto the trigonal axis of the crystal are $O_1O_2 = 3.05$ Å, $O_3O_4 = 2.40$ Å. ●) Cu^{2+}, ○) H_2O.

are three times as numerous as the particular sites, which are located on the threefold axis and are occupied by undistorted octahedra (Fig. 2). The symmetry of the static distortions of the octahedral copper complexes is triclinic, but it is close to the tetragonal symmetry characteristic for the Jahn–Teller effect. The normals to the faces of the distorted $[Cu(H_2O)_6]^{2+}$ octahedra in the general sites do not coincide with the direction of the trigonal axis of the crystal, and as a result the projection of these complexes onto the trigonal axis is larger than for the undistorted complexes found in the particular sites (Fig. 1). In the high-symmetry phase PI all the octahedral copper complexes are undistorted and, just as for the particular sites in PII, the trigonal axes of the $[Cu(H_2O)_6]^{2+}$ complexes are parallel to the trigonal axis of the crystal. At the PI–PII phase transition the appearance of two types of octahedra causes a doubling of the period a, with $a/2$ and c in the PII phase being 2.4% smaller and 2.4% larger, respectively, than the periods a and c in PI. The copper-oxygen distances in the regular copper octahedra in PI and PII are 2.193 and 2.074 Å, respectively; for the octahedra in particular sites in PII this distance is approximately equal to the mean value of the semi-axes of the distorted octahedra in the general sites. These structural data, in conjunction with the data from studies of $[Cu(H_2O)_6]^{2+}$ impurity complexes in fluosilicates,[8] indicate that the probable cause of the phase transition is the cooperative Jahn–Teller effect. Structural and calorimetric studies of solid solutions based on $CuSiF_6 \cdot 6H_2O$ have revealed[4] another structural phase transition at 260 K to a low-temperature phase PIII. The temperature of the PIII–PII transition upon heating is 275 K. It is important for the studies reported in the present article that the PII–PIII phase transition does not occur during cooling at rates above 50 K/min.

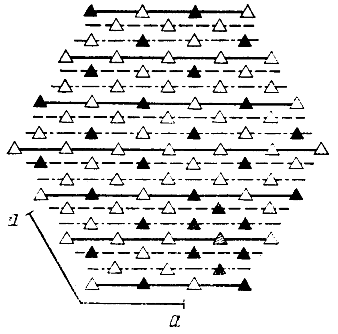

FIG. 2. Projections of the cation sublattice of the PII phase of $CuSiF_6 \cdot 6H_2O$ onto a plane perpendicular to the trigonal axis: ▲) regular $[Cu(H_2O)_6]^{2+}$ complexes in particular sites; △) distorted $[Cu(H_2O)_6]^{2+}$ complexes in general sites; a is the lattice period in the plane, c the period along the trigonal axis. The planes in which the complexes are joined by the solid, dot-and-dash, and dashed lines are located successively a distance $\frac{1}{3}c$ from one another along the trigonal axis. The impurity complex $[Fe(H_2O)_6]^{2+}$ (the hatched triangle) is located in a cluster with disordered distortions.

3. PREPARATION OF SAMPLES AND MEASUREMENT TECHNIQUES

The Mössbauer method was used to study the solid solutions $Cu_{1-x}{}^{57}Fe_xSiF_6 \cdot 6H_2O$ based on $CuSiF_6 \cdot 6H_2O$. The samples were grown by crystallization from an aqueous solution at a temperature of 14 ± 0.05 °C. It turned out not to be possible to prepare small quantity (tens of milligrams) of $^{57}FeSiF_6 \cdot 6H_2O$ by dissolution of ^{57}Fe-enriched metallic iron in fluosilicic acid, because even in the presence of a protective medium (hydrogen) the iron was oxidized to the trivalent state. For this reason the iron was introduced into a solution of $CuSiF_6 \cdot 6H_2O$ not in the form of a salt but as a finely disperse metallic powder obtained from ferric oxide by reduction with hydrogen. As a result of the reaction, the $^{57}Fe^{2+}$ ions went into solution with the copper fluosilicate, replacing the copper. The finely disperse powder made for a rapid and complete dissolution of the iron. The structure of the resulting single crystals of $Cu_{1-x}{}^{57}Fe_xSiF_6 \cdot 6H_2O$ ($x \lesssim 0.05$) was monitored by x-ray diffraction and corresponded to the structure of the PII phase of $CuSiF_6 \cdot 6H_2O$. The Mössbauer studies were carried out on polycrystalline samples which were hermetically sealed in a polymethylmethacrylate cell to prevent loss of their water of crystallization. A helium cryostat with an exchange gas was used in the experiments. This circumstance, and also the fact the sample was placed between beryllium plates, minimized the temperature gradient across the sample. The temperature was maintained to within 0.05 K. The use of a resonance detector based on a ^{57}Fe–Al alloy increased the magnitude of the effect and the resolution of the experiment. The Mössbauer absorption spectra for 14.4 keV γ rays (the source was ^{57}Co in Pd) were measured in a constant-acceleration spectrometer in which the velocity change was described by a triangular law. The mirror-image halves of the spectrum were added together to reduce the geometric effect, and further processing was done on a computer.

4. MAIN RESULTS OF THE EXPERIMENT

In order to study the PII phase over a wide range of temperature, we made use of the circumstance that the PII-PIII transition does not occur on rapid cooling of PII. On slow cooling, owing to the presence of thermal hysteresis, the PII phase exists down to a temperature $T = 260$ K. The Mössbauer spectra of samples cooled from $T = 300$ K to temperatures of 78 and 4.2 K at rates in excess of 50 K/min consist of a quadrupole doublet with unbroadened lines (half-width $\Gamma \approx 0.23$ mm/sec), indicating that the two structurally inequivalent sites of the iron ions which replace cop-

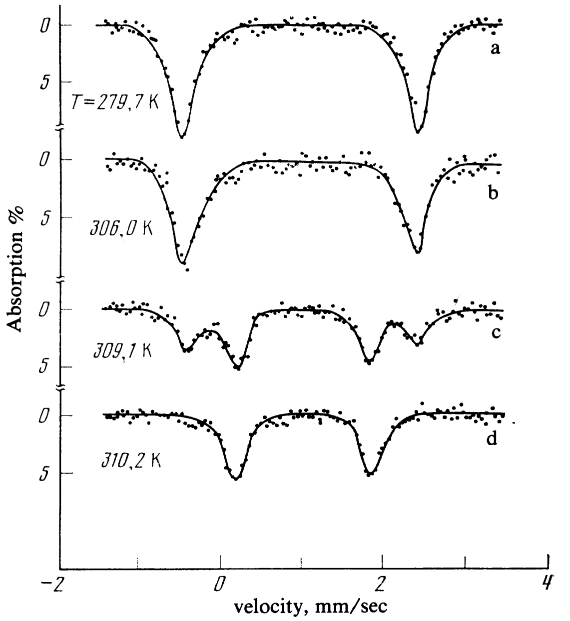

FIG. 3. Mössbauer spectra of $^{57}Fe^{2+}$ impurity ions in $Cd_{1-x}Fe_xSiF_6\cdot 6H_2O$ in the PII–PI phase transition region.

per in the cation sublattice of the PII phase are indistinguishable at these temperatures. On increasing temperature in the interval 270–290 K the spectral lines begin to broaden, and above 290 K there is a noticeable asymmetry in the lines of the quadrupole doublet (Fig. 3b). To increase the reliability of the results the experimental data were processed using two different minimization methods—coordinate[9] and gradient.[10] The data obtained by applying these algorithms are in qualitative agreement. For $T<290$ K the insufficient resolution causes large errors of approximation, and the actual errors are larger than those shown in Fig. 4 because the result of the fitting is correlated with the initial data. For $T\geqslant 290$ K the representation of the spectrum as two quadrupole doublets with different temperature dependences of the quadrupole splitting corresponds to smaller values of the functional (Fig. 4). The intensity ratio S_i/S_e of the spectra with the smaller (ΔE_i) and the larger (ΔE_e) values of the splittings in the interval 280–295 K is close to $\frac{1}{3}$ (Fig. 5a), which corresponds to the ratio of the number of $[Cu(H_2O)_6]^{2+}$ complexes in the particular and general sites of the cation sublattice. This gives us reason to suppose that the quadrupole doublets with ΔE_i and ΔE_e correspond to iron ions replacing copper in the particular and general sites of the cation sublattice. At $T=300$ K we have $\Delta E_e = 1.52 \pm 0.02$ mm/sec and $\Delta E_i = 2.66 \pm 0.03$ mm/sec, and for the isomer shift we have $\delta_e = 1.52 \pm 0.02$ mm/sec and $\delta_i = 1.45 \pm 0.02$ mm/sec (relative to sodium nitroprusside). The reliability of the results for $T\geqslant 290$ K will be confirmed later on by comparing them with data for isomorphous fluosilicates.

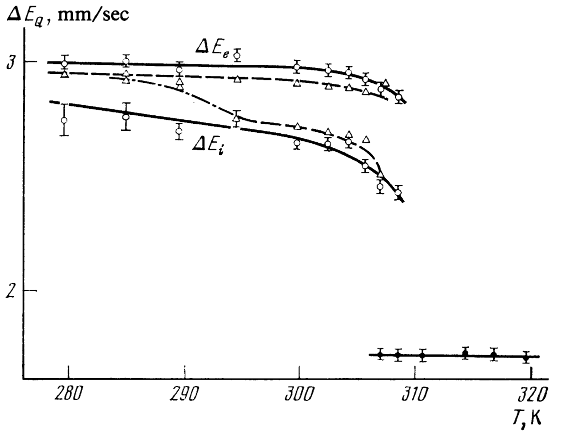

FIG. 4. Temperature dependence of ΔE_Q for $^{57}Fe^{2+}$ impurity ions at the phase transitions: △) values obtained by the method of coordinate descent; ○) values obtained by the method of gradient descent; in the PI phase the two methods give the same results.

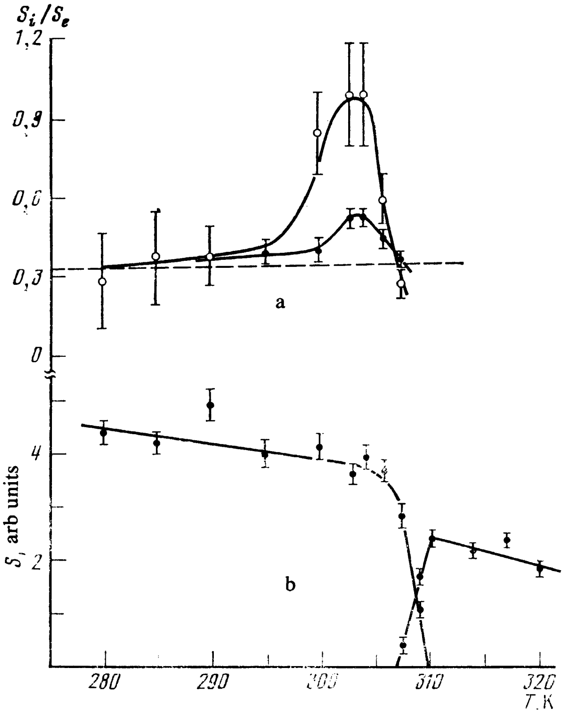

FIG. 5. Temperature dependence of the intensity ratio (a) and ratio of the areas under the resonance absorption spectrum (b): ●) values obtained by the method of coordinate descent; ○) values obtained by the method of gradient descent.

In the interval 295–305 K the relative intensity of the lines corresponding to the particular sites reaches a maximum at $T=305$ K. It should be stressed that in this temperature interval the sample is in a single phase. The PI phase is observed to arise at $T=307$ K, in agreement with the x-ray diffraction data. The phase transition is complete at $T=310$ K. The linwidth in PI is close to the instrumental width ($\Gamma \approx 0.23$ mm/sec), the quadrupole splitting is $\Delta E_Q = 1.73 \pm 0.02$ mm/sec ($T=300$ K), and the isomer shift relative to sodium nitroprusside is 1.51 ± 0.01 mm/sec ($T=300$ K). The PII–PI phase transition is accompanied by a decrease in the area under the resonance absorption spectrum (Fig. 5b), in agreement with the larger specific volume of the high-temperature phase PI relative to PII.

5. DISCUSSION OF RESULTS

The experimental results can be explained qualitatively on the basis of a microscopic model for the cooperative Jahn–Teller effect. Taking the case of an E–e term and a strong vibronic coupling, and neglecting the tunneling splitting, one finds a suitable choice in the three-states Potts model.[11] According to this model, one assigns to each Jahn-Teller complex at a lattice site a certain value of the vector $Q=\begin{pmatrix}Q_3\\Q_2\end{pmatrix}$. The coordinates Q_3 and Q_2 of this vector describe the Jahn-Teller distortion of the complexes and form the basis of a two-dimensional irreducible representation E_{2g} of the symmetry group of the octahedron. In the case of strong vibronic coupling the distortions are localized near one of the three equivalent minima of the adiabatic potential, and therefore the vector $\mathbf{Q}$ can assume only one of three fixed values

$$\mathbf{Q}_x=\begin{pmatrix}-1/2\\ \sqrt{3}/2\end{pmatrix},\quad \mathbf{Q}_y=\begin{pmatrix}-1/2\\ -\sqrt{3}/2\end{pmatrix},\quad \mathbf{Q}_z=\begin{pmatrix}1\\0\end{pmatrix},$$

corresponding to tetrahegonal extensions of the octaheda along the fourfold symmetry axes, which correspond to the axes of the Cartesian coordinate system.

In the presence of a bilinear interaction between the distortions of nearest neighbors the model Hamiltonian is of the form

$$\mathrm{H}=-\frac{1}{2}\sum_{i,j}\mathbf{Q}_i\hat{V}_{ij}\mathbf{Q}_j, \tag{1}$$

where $\hat{V}_{ij}$ is the interaction matrix for a pair of octahedra joined by lattice vector $\mathbf{r}_{ij}$. The ferrodistortive and antiferrodistortive orderings in model (1) for the case of a sample cubic lattice were investigated in Ref. 11, where it was pointed out that more complex low-temperature structures are possible. In particular, there is a possible ordering described by normal modes with the star of wave vectors

$$\mathbf{k}_1=(^1/_2,\ ^1/_2,\ 0),\quad \mathbf{k}_2=(0,\ ^1/_2,\ ^1/_2),\quad \mathbf{k}_3=(^1/_2,\ 0,\ ^1/_2).$$

The phase transition in such a structure has not been considered before, and we shall therefore describe its main features in the framework of molecular field theory. This case corresponds to a four-sublattice model: The simple cubic lattice is separated into four interpenetrating body-centered lattices, each of which is assigned an average value of the vector $\mathbf{Q}$. In this model the free energy of the system is

$$\mathcal{F}=-\frac{N}{4}\sum_{i,j}\langle\mathbf{Q}\rangle_i\hat{V}_{ij}\langle\mathbf{Q}\rangle_j+\frac{1}{4}TN\times\sum_{i=1}\sum_{\alpha=x,y,z}\frac{1+2\langle\mathbf{Q}\rangle_i\mathbf{Q}_\alpha}{3}\ln\frac{1+2\langle\mathbf{Q}\rangle_i\mathbf{Q}_\alpha}{3}, \tag{2}$$

where $\langle\mathbf{Q}\rangle_i$ is the average value of the vector $\mathbf{Q}$ is the ith sublattice;

$$V_{ij}=\hat{V}_{ji}=\begin{pmatrix} v_\parallel\cos^2\varphi+v_\perp\sin^2\varphi & ^1/_2(v_\parallel-v_\perp)\sin 2\varphi\\ ^1/_2(v_\parallel-v_\perp)\sin 2\varphi & v_\parallel\sin^2\varphi+v_\perp\cos^2\varphi\end{pmatrix},$$

$$\varphi=\begin{cases}0\,(i,j)=(1,4);\ (2,3)\\ ^2/_3\pi\,(i,j)=(1,2);\ (3,4);\\ -^2/_3\pi\,(i,j)=(1,3);\ (2,4)\end{cases}$$

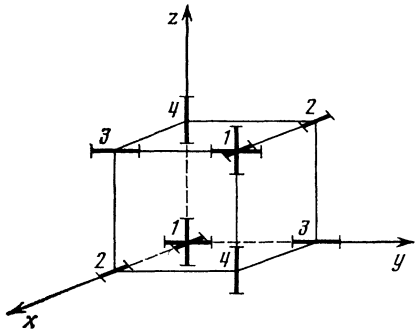

FIG. 6. Primitive cell of the disordered phase. The numbers indicate the sublattice, and the line segements represent the distortions of the octahedra in the ordered phase. To obtain the rhombohedral structure of $CuSiF_6{\cdot}6H_2O$, compress the pictured cube along the 1–1 diagonal without changing the directions of the distortions.

$v_\parallel$ and $v_\perp$ are the constants for the binary interaction of distortions, T is the absolute temperature expressed in energy units, and N is the number of interacting complexes.

In the case of a rhombohedral lattice expression (2) remains valid if one considers the following remarks. First, a rhombohedral lattice can be obtained from a cubic lattice by a continuous deformation which preserves the orientation of the Cartesian coordinate system tied to the octahedra (Fig. 6). Second, the four equivalent sublattices of the rhombohedral lattice are also rhombohedral, since a body-centered rhombohedral lattice can be reduced to a simple one. Third, the crystalline field of a rhombohedral lattice causes additional distortions of the octahedra. These distortions have a trigonal asymmetry and transform according to irreducible representation T_{2g} of the group O_h, and so to first approximation they do not interact with the Jahn-Teller coordinates Q_3, Q_2 and can be dropped from consideration here. Fourth, the lowering of the symmetry of the lattice relaxes the restrictions on the matrices $\hat{V}_{ij}$ and, generally speaking, complicates their form. In the present case, however, this does not occur, since the symmetry group of the vector $\mathbf{r}_{ij}$ joining the pair of nearest neighbors is C_{2h} (this group also includes the transformations taking $\mathbf{r}_{ij}$ into $-\mathbf{r}_{ij}$). The group C_{2h} contains the rotation C_2 whose matrix in the E_{2g} representation is $\hat{D}(C_2)=\begin{pmatrix}1&0\\0&-1\end{pmatrix}$, and the symmetry condition[11]

$$\hat{D}(C_2)\hat{V}_{14}\hat{D}^{-1}(C_2)=\hat{V}_{14},\qquad \hat{D}(C_2)\hat{V}_{23}\hat{D}^{-1}(C_2)=\hat{V}_{23}$$

leads to a diagonal form for the matrices $\hat{V}_{14}$, $\hat{V}_{23}$, while the remaining matrices $\hat{V}_{ij}$ can all be obtained from these two by rotations about the C_3 axis, as in the case of a cubic lattice. Therefore, the matrices $\hat{V}_{ij}$ for the cubic and rhombohedral lattices have the same form. One can easily verify that the condition of minimum free energy $\partial\hat{\mathcal{F}}/\partial\langle Q\rangle_i=0$ is satisfied by the solution

$$\langle\mathbf{Q}_1\rangle=0,\quad \langle\mathbf{Q}\rangle_2=\zeta Q_x,\quad \langle\mathbf{Q}\rangle_3=\zeta\mathbf{Q}_y,\quad \langle\mathbf{Q}\rangle_4=\zeta\mathbf{Q}_z. \tag{3}$$

What we have found for the character of the distortions agrees with the x-ray diffraction data, and this confirms the validity of the four-sublattice model for the case under consideration. Sublattice 1 corresponds to the particular sites, while the general sites belong to sublattices 2, 3, and 4 (Fig.

6). The function $\zeta(T)$ has two branches: the first is $\zeta(T) \equiv 0$ and the second is given implicitly by

$$3\zeta = \tau[\ln(1+2\zeta) - \ln(1-\zeta)], \tag{4}$$

where $\tau = 2T/(-3v_\perp + v_\parallel)$ is the reduced temperature. The first branch corresponds to the minimum for $\tau > 1$, while the second exists for $0 < \tau < \tau_+ \approx 1.09$. The equilibrium phase transition occurs under the condition $\mathscr{F}(\zeta = 0) = \mathscr{F}(\zeta \neq 0)$, from which, with allowance for (2)–(4), we find the phase transition temperature and the discontinuity of the order parameter $\zeta(\tau_0)$:

$$\tau_0 \approx 1.08, \quad \zeta(\tau_0) = 0.5.$$

The overlap of the existence regions of the two types of solutions $\zeta(\tau_0)$ indicates that the phase transition is first-order, in agreement with the experimental data and the result of the phenomenological theory.[5,6] The fact that our model gives a pretransitional anomaly of the temperature dependence of the specific heat (a square-root divergence near τ_+) that agrees with calorimetry experiments[6] allows us to apply the ideas set forth above to the description of the pretransitional changes in the Mössbauer spectra as well.

The quadrupole splitting

$$\Delta E_Q \sim V_{zz}(1 + {}^1/_3\eta^2)^{1/2} \tag{5}$$

observed in the Mössbauer spectra is related to the electric-field-gradient tensor

$$\begin{pmatrix} V_{xx} & 0 & 0 \\ 0 & V_{yy} & 0 \\ 0 & 0 & V_{zz} \end{pmatrix},$$

which, in turn, is determined by the distortions of the complex containing the $^{57}Fe^{2+}$ impurity center. The asymmetry parameter is $\eta = (v_{xx} - V_{yy})/V_{zz}$. In the fluosilicates $MeSiF_6 \cdot 6H_2O$ (Me = Zn, Ni, Co) with space group $R\bar{3}$ (Ref. 12) the intracrystalline field has axial symmetry.[13] The orbital ground state of the impurity ion Fe^{2+} in these compounds and in the $R\bar{3}m$ fluosilicates (Me = Fe, Mn, Mg; Ref. 14)[1)] is a singlet,[13,16] with the $[Fe(H_2O)_6]^{2+}$ octahedra elongated[14] along their trigonal axis, which coincides with the rhombohedral axis of the crystal.[13,16] This deformation of the $[Fe(H_2O)_6]^{2+}$ octahedron is due to both the interaction of the iron ion with its ligands and the interaction of the iron ion of the impurity octahedron with the host lattice.

It is possible that the trigonal distortions of the iron complex in fluosilicates can be explained as the realization of the trigonal extrema of the $T-(e+t_2)$ problem[17] in the crystalline field. However, unlike that of the E term, the Jahn–Teller effect for the T term is less significant, since the coefficient of the complex is stabilized by the spin-orbit interaction,[18] and the ground state of the ion is formed by nonbonding electrons.[19] Therefore, the main factor influencing the deformation of the $[Fe(H_2O)_6]^{2+}$ complex is evidently the interaction with the host lattice. In this case the trigonal deformation of the iron impurity complex and, consequently, the quadrupole splitting should depend on the lattice parameters. Let us specify this dependence more concretely.

According to Refs. 20 and 21 the quadrupole splitting at a $^{57}Fe^{2+}$ nucleus in an octahedral coordination is determined by the coefficient of the valence electrons of the $^5T_{2g}$ term and the lattice charges. In the case of fluosilicates the latter contribution is less than 0.02 mm/sec and can be neglected.[22] In the axially symmetric case

$$\Delta E_Q \sim V_{zz} \sim F(\delta, \lambda, T), \tag{6}$$

where $F(\delta, \lambda, T)$ is the Ingalls function, which depends on the temperature T, the size of the splitting of the $^5T_{2g}$ term in the axial field, and the covalency factor α_2: $\lambda = \alpha^2\lambda_0$ ($\lambda_0 = -103$ cm^{-1}). Following the calculations of Ref. 20, one can show that for a singlet ground state ($\delta < 0$) and for ratios $\delta/\lambda < 4$, as are characteristic for $R\bar{3}$ fluosilicates, one has in the temperature interval 4.2–300 K

$$F(\delta, \lambda, T) \sim \delta. \tag{7}$$

The size of the splitting δ can be determined from the deformation of the $[Fe(H_2O)_6]^{2+}$ complex along the z axis[23]:

$$\delta \sim \sin(\beta - \beta_0), \tag{8}$$

where β is the angle between the z axis of the $[Fe(H_2O)_6]^{2+}$ complex and the direction from the center to the vertex of the octahedron ($\beta_0 = 54°44'$ in the undistorted octahedron). The size of the trigonal deformation (8) of the complex is determined by its interaction with the nearest-neighbor environment. For complexes belonging to the cation sublattice this is a pair of $[SiF_6]^{2-}$ octahedra belonging to the anion sublattice and located along the trigonal axis. According to x-ray diffraction studies[7] and direct measurements of the compliance along ($\sigma_\parallel$) and perpendicular to ($\sigma_\perp$) the trigonal axis in fluosilicates ($\sigma_\perp/\sigma_\parallel = 2.56$ in $ZnSiF_6 \cdot 6H_2O$),[24] the stiffness of the hydrogen bonds of the complexes in a "column" is substantially greater than that of the bonds between "columns." Therefore, the influence of the next nearest neighbors (of the second coordination sphere of the anion sublattice) on the deformation of the $[Fe(H_2O)_6]^{2+}$ impurity complexes can be neglected. We thus conclude that the deformation of the $[Fe(H_2O)_6]^{2+}$ octahedron should depend mainly on the lattice period c along the trigonal axis of the crystal.

Let us denote by c_0 the lattice period along the trigonal axis for a hypothetical fluosilicate crystal containing undistorted $[Fe(H_2O)_6]^{2+}$ impurity complexes. Then

$$\sin(\beta - \beta_0) \sim (c - c_0). \tag{9}$$

Taking it into account that the covalency factors of all fluosilicates are about the same, we obtain the equation

$$\Delta E_Q = \gamma_1 c + \gamma_2, \tag{10}$$

which relates the quadrupole splitting at $^{57}Fe^{2+}$ impurity nuclei, as measured at a definite temperature, to the lattice period c along the trigonal axis of the crystal. The linear nature of Eq. (10) is confirmed by the experimental data (Fig. 7). In the analogous dependence of ΔE_Q on the lattice period a in a hexagonal setting, no correlation is observed between the quadrupole splitting and this period (except in cases where c/a = const). We note that for $R\bar{3}$ and $R\bar{3}m$ fluosilicates the constants γ_1 and γ_2 are different. The linear nature of Eq. (10) also agrees with the data of Ref. 25, which imply a linear dependence of the quadrupole splitting on the iron concentration in the solid solution $Zn_{1-x}{}^{57}Fe_xSiF_6 \cdot 6H_2O$.

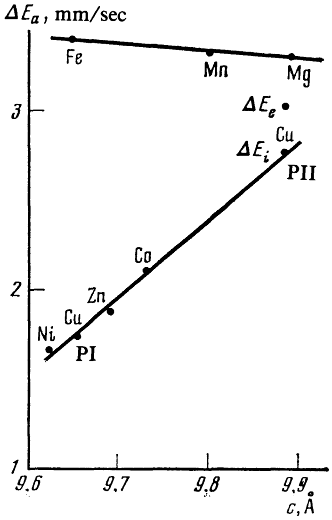

FIG. 7. ΔE_Q at the $^{57}Fe^{2+}$ impurity ions (concentration of $\lesssim 1\%$) in Me-$SiF_6{\cdot}6H_2O$ fluosilicates (Me = Ni, Cu, Zn, Co, Fe, Mn, Mg) *versus* the lattice period c ($T = 300$ K). The value of ΔE_Q for copper fluosilicate was obtained in the present study; the values for the other fluosilicates are found in Ref. 26.

Besides the trigonal field of the lattice, the distortion of the $[Fe(H_2O)_6]^{2+}$ octahedra is affected by the field of the tetragonal distortions of the neighboring copper-centered octahedra. This field for the l th impurity complex

$$U(\mathbf{Q}_l) = -\frac{1}{2}\mathbf{Q}_l\sum_j \hat{V}_{lj}\langle\mathbf{Q}_j\rangle$$

(the sum is over nearest neighbors of the l th octahedron) is linear in the coordinates of the tetragonal distortions Q_3 and Q_2, and it therefore shifts the trigonal minimum of the potential to nonzero values of the tetragonal coordinates, i.e., imposes tetragonal distortions. This leads to a nonaxial character of the electric field of the ligands: $V_{xx} \neq V_{yy}$, and therefore the quadrupole splitting (5) of an octahedron which is distorted both trigonally and tetratonally is greater than that of an octahedron which is distorted only trigonally.

In the particular sites the copper octahedra have $\langle\mathbf{Q}\rangle = 0$, and so they are distorted along the x, y, or z axis with equal probability. The question of whether these distortions are dynamic or static can be answered, we believe, by the experiments described above, and we shall say more about this below. In the general sites the copper octahedra have static distortions proportional to $\mathbf{Q}_x$, $\mathbf{Q}_y$, and $\mathbf{Q}_z$, respectively. The mean field of the distortions due to the nearest neighbors zero is in the particular sites and proportional to $\mathbf{Q}_x$, $\mathbf{Q}_y$, $\mathbf{Q}_z$ in the general sites. Therefore, the mean distortions of the impurity octehedra in the particular sites are purely trigonal and in the general sites consist of a sum of trigonal and tetragonal distortions. As a result, the Mössbauer spectra should contain two doublets, with the inner doublet corresponding to the particular sites and the outer doublet to the general sites. In fact, the experimental quadrupole splitting for iron ions in particular sites in phase PII agrees with Eq. (10) (see Fig. 7); consequently, the crystalline field in the particular sites at $T = 300$ K has axial symmetry. An analogous conclusion follows for a high-temperature phase PI whose lattice period is obtained by extrapolating the concentration dependence of the period to zero impurity concentration. The value of the quadrupole splitting in the general sites in PII for $T = 300$ K is larger than in the particular sites, indicating that the crystalline field in the general sites is nonaxial.

At low temperatures, however, one sees only a single pair of lines. This circumstance can be attributed to the presence of tetragonal distortions of the octahedra in the particular sites as well. If the lifetime of such distortions is shorter than the lifetime τ of the nucleus in the excited state ($\tau \approx 10^{-7}$ sec), then they will in fact be detected in Mössbauer experiments. Tetragonal distortions of the impurity octahedra in particular sites in PII could be caused by an interaction with $[Cu(H_2O)_6]^{2+}$ octahedra, also in particular sites, which are located on the diagonals of the primitive cell of the high-temperature phase and are statically disordered—these are the first (of course, non-nearest) neighbors which give a nonzero contribution to the tetragonal-distortion potential for the particular sites. With increasing temperature the frequency of the dynamic distortions of the $[Cu(H_2O)_6]^{2+}$ octahedra in the particular sites increases and, consequently, the asymmetry parameter η decreases. As a result, the quadrupole splittings in the particular and general sites begin to differ, and the spectral lines become asymmetric (Fig. 3b). When the frequency of the dynamic distortions of the complexes significantly exceeds 10^7 Hz, the quadrupole splitting in the particular sites will correspond to Eq. (10) for an axially symmetric crystalline field. In the disordered phase the quadrupole splitting corresponds to an axial character of the field at the nucleus, and this indicates that the frequency of the distortions of the $[Cu(H_2O)_6]^{2+}$ complexes exceeds 10^7 Hz. In the opposite case, and also in the presence of disordered static distortions, the interaction with the distortions of nearest-neighbor complexes located along the trigonal axis of the crystal would lead to a finite value of the asymmetry parameter.

The area ratio of the quadrupole doublets corresponding to the particular and general sites is given by

$$S_i/S_e = N_i f_i / N_e f_e, \qquad (11)$$

where N_i and N_e are the numbers of iron atoms in particular and general sites, and f_i and f_e are the Mössbauer-effect probabilities in these sites. In the interval 280–295 K the quantity S_i/S_e approximately coincides with the ratio of the numbers of particular and general sites in PII, equal to $\frac{1}{3}$. The assumption that the iron is distributed with equal probability over the particular and general sites in the cation sublattice of the crystal implies equal probabilities for the effect in the particular and general sites of the PII phase for $T < 295$ K. The increase in the relative intensity of the doublet corresponding to an axial field at the nucleus in the temperature interval 295–305 K indicates that completely disordered clusters with the structure characteristic of the high-temperature phase form in PII near the point of the phase transition. In the clusters the correlation of the distortions disappears, and the field at the nucleus of the

$[Fe(H_2O)_6]^{2+}$ impurity complexes becomes axial (Fig. 2). The area ratio S_i/S_e therefore grows to more than $\frac{1}{3}$.

We note that in the above discussions we could not consider only the mean values of the distortions but had to take fluctuations into account. This is because the averaging time in Mössbauer experiments is short ($\approx 10^{-7}$ sec), and deviations from the mean values that occur over times longer than 10^{-7} sec are all perceived as static.

At temperatures above $T = 300$ K a progressive decrease is observed in the quadrupole splitting at the sites of the cation sublattice; this decrease is correlated, in accordance with Eq. (10), with a decrease in the lattice period along the trigonal axis of the crystal, as is revealed by x-ray diffraction studies in this same temperature interval. The decrease in the lattice period could be caused by rotations of the copper octahedral complexes at general sites to the positions which they occupy in PI. Rotations of the $[Cu(H_2O)_6]^{2+}$ octahedra cause the projection of these octahedra onto the trigonal axis of the crystal to decrease, and, consequently, the lattice period of the crystal along the trigonal axis decreases. There is a simultaneous increase in the projection of the complex in the orthogonal direction, and the lattice period a increases. When the lattice period c decreases there is a compression of the columns of $[Cu(H_2O)_6]^{2+}$ octahedra, but rotations of the copper complexes occur only in the columns corresponding to the general sites of the cell. Therefore, the compression of the $[Fe(H_2O)_6]^{2+}$ complexes is greater in the columns corresponding to particular sites, and this makes for a greater decrease in ΔE_Q in the particular sites (Fig. 4). Estimates show that the rotations of the copper complexes in the general sites cannot cause an anomalous growth of the specific volume of the unit cell of PII in the pretransition region. The anomalous growth of the specific volume of PII is probably caused by an increase, occurring simultaneously with the increase in the frequency of the Jahn-Teller distortions, in the dimensions of the dynamically regular copper complexes. A comparison of the copper-oxygen distance in PI with that for the particular sites in PII is consistent with this conclusion. The formation of clusters with disordered distortions of the complexes, the rotations of the $[Cu(H_2O)_6]^{2+}$ octahedra in the general sites of the unit cell, the increase in the frequency of dynamic Jahn-Teller distortions of the copper complexes, and the increase in the effective dimensions of these complexes begin to occur in the low-temperature phase PII. Thus at the first-order phase transition in the crystals under study there occurs, in the framework of the initial phase, a motion of the elements of structure toward states which are peculiar to the new phase.

We are grateful to S. I. Reĭman for assistance in processing the experimental results.

[1)] Refinements to the structure of $MeSiF_6 \cdot 6H_2O$ (Me = Fe, Mn, Mg) may be found in Ref. 15.

[1] B. S. Bokshteĭn, Yu. B. Voĭtkovskiĭ, G. S. Nikol'skiĭ, and I. M. Razumovskiĭ, Zh. Eksp. Teor. Fiz. **64**, 553 (1973) [Sov. Phys. JETP **37**, 283 (1973)]; B. S. Bokshteĭn, L. N. Klinger, and I. M. Razumovskiĭ, Fiz. Tverd. Tela (Leningrad) **19**, 476 (1977) [Sov. Phys. Solid State **19**, 274 (1977)].

[2] Chen Hayden and J. B.Cohen, Metall. Trans. A **12**, 575 (1981).

[3] Ya. A. Kraftmakher, in: Fizika Tverdogo Tela i Termodinamika [Solid-State Physics and Thermodynamics], Nauka Novosibirsk (1971), p. 68; Ya. A. Kraftmakher and P. G.Strelkov, Fiz. Tverd. Tela (Leningrad) **8**, 1049 (1966) [Sov. Phys. Solid State **8**, 838 (1960)].

[4] G. Ya. Sukharevskiĭ, F. A.Boĭko, A. M. Bykov, V. E. Ganenko, E. O. Tsybul'skiĭ, and G. E. Shatalova, Dokl. Akad. Nauk SSSR **256**, 1390 (1981) [Sov. Phys. Dokl. **26**, 131 (1981)].

[5] B. Ya. Sukharevskiĭ, E. O. Tsybul'skiĭ, G. E. Shatalova and I. M. Vitebskiĭ, Kristallografiya **28**, 488 (1983) [Sov. Phys. Crystallogr. **28**, 288 (1983)]; E. O. Tsybul'skiĭ, B. Ya. Sukharevskiĭ, G. E. Shatalova, and N. E. Pis'menova, Preprint No. 52, Physicotechnical Institute, Academy of Sciences of the Ukrainian SSR, Donetsk (1982).

[6] B. Ya. Sukharevskiĭ, F. A. Boĭko, A. M. Bykov, I. M. Vitebskiĭ, and V. E. Ganenko, Dokl. Akad. Nauk SSSR **266**, 93 (1982) [Sov. Phys. Dokl. **27**, 730 (1982)].

[7] S. Ray, A. Zalkin, and D. H. Templeton, Acta Crystallogr. Sect. B **29**, 2748 (1973).

[8] B. Bleaney, K. D. Bowers, and R. S. Trenam, Proc. R. Soc. London Ser. A **228**, 157 (1955); H. M. L. Pryce and A. Abragam, Proc. Phys. Soc. A **63**, 409 (1950).

[9] V. G. Karmanov, Matematicheskoe Programmirovanie [Mathematical Programming], Nauka, Moscow (1975), p. 272.

[10] V. D. Checherskiĭ and V. P. Romanov, Preprint No. 15–77, Physicotechnical Inst. of Low Temperatures, Academy of Sciences of the Ukrainian SSR, Kharkov (1977), p. 56.

[11] K.-H. Höck, G. Schröder, and H. Thomas, Z. Phys. B **30**, 403 (1978).

[12] S. Ray, A. Zalkin, and D. H. Templeton, Acta Crystallogr. Sect. B **29**, 2741 (1973).

[13] J. Chappert, G. Jehanno, and F. Varret, J. Phys. (Paris) **38**, 411 (1977).

[14] W. Hamilton, Acta Crystallogr. **15**, 353 (1962); E. Kodera, A. Torii, K. Osaka, and T. Watanabe, J. Phys. Soc. Jpn. **32**, 863 (1972); S. Syoyama and K. Osaka, Acta Crystalogr. Sect. B **28**, 2626 (1972).

[15] G. Chevrier, A. Hardy, and G. Jehanno, Acta Crystallogr. Sect. A **37**, 578 (1981); G. Chevrier and G. Jehanno, Acta Crystallogr. Sect. A **35**, 912 (1979); G. Jehanno and F. Varret, Acta Crystallogr. Sect. A **31**, 857 (1975).

[16] F. Varret and J. Danon, Chem. Phys. Lett. **20**, 538 (1973); V. K. Garg and K. Chandra, Phys. Status Solidi B **50**, K49 (1972).

[17] I. B. Bersuker and V. Z. Polinger, Vibronnye Vzaimodeĭstviya v Molekulakh i Kristallakh [Vibronic Interactions in Molecules and Crystals], Nauka, Moscow (1983), Sec. 6.

[18] J. H. Van Vleck, Physica (Utrecht) **26**, 544 (1960).

[19] C. J. Ballhausen, Introduction to Ligand Field Theory, McGraw-Hill, New York (1962) [Russian translation Mir, Moscow (1964), p. 257].

[20] R. Ingalls, Phys. Rev. **133**, A787 (1964).

[21] R. Zimmermann and H. Spiering, Phys. Status Solidi B **67**, 487 (1975).

[22] A. J. Nozik and M. Kaplan, Phys. Rev. **159**, 273 (1967).

[23] J. Pebler, D. Reinen, K. Schmidt, and F. Steffens, J. Solid State Chem. **25**, 107 (1978).

[24] V.I. Vasyukov, S. N. Lukin, and G. A. Tsintsadze, Zh. Eksp. Teor. Fiz. **77**, 1544 (1979) [Sov. Phys. JETP **50**, 774 (1979)].

[25] F. Varret, J. Danon, P. Imbert, and G. Jehanno, J. Phys. (Paris) **35**, C1-87 (1974).

[26] F. Varret and G. Jeganno, J. Phys. (Paris) **35**, C6-639 (1974).

Translated by Steve Torstveit